**Paul C. Herrmann[1]**
**John W. Gillespie[1]**
**Lu Charboneau[1]**
**Verena E. Bichsel[2]**
**Cloud P. Paweletz[1]**
**Valerie S. Calvert[2]**
**Elise C. Kohn[1]**
**Michael R. Emmert-Buck[1]**
**Lance A. Liotta[1]**
**Emanuel F. Petricoin III[2]**

[1]FDA-NCI Clinical Proteomics Program, Laboratory of Pathology, NIH, Bethesda, MD, USA
[2]FDA-NCI Clinical Proteomics Program, Division of Therapeutic Products, FDA, Bethesda, MD, USA

# Mitochondrial proteome: Altered cytochrome *c* oxidase subunit levels in prostate cancer

Laser capture microdissection was combined with reverse phase protein lysate arrays to quantitatively analyze the ratios of mitochondrial encoded cytochrome *c* oxidase subunits to nuclear encoded cytochrome *c* oxidase subunits, and to correlate the ratios with malignant progression in human prostate tissue specimens. Cytochrome *c* oxidase subunits I-III comprise the catalytic core of the enzyme and are all synthesized from mitochondrial DNA. The remaining subunits (IV–VIII) are synthesized from cellular nuclear DNA. A significant ($P < 0.001$, 30/30 prostate cases) shift in the relative concentrations of nuclear encoded cytochrome *c* oxidase subunits IV, Vb, and VIc compared to mitochondrial encoded cytochrome *c* oxidase subunits I and II was noted during the progression of prostate cancer from normal epithelium through premalignant lesions to invasive carcinoma. Significantly, this shift was discovered to begin even in the premalignant stage. Reverse phase protein lysate array-based observations were corroborated with immunohistochemistry, and extended to a few human carcinomas in addition to prostate. This analysis points to a role for nuclear DNA encoded mitochondrial proteins in carcinogenesis; underscoring their potential as targets for therapy while highlighting the need for full characterization of the mitochondrial proteome.

**Keywords:** Cancer / Cytochrome *c* oxidase / Mitochondrial proteome / Oxidative phosphorylation / Prostate
PRO 0461

## 1 Introduction

Differences in cellular metabolism between normal and neoplastic tissue have attracted considerable interest since the proposal by Warburg in the 1920s that some cell types decrease oxidative phosphorylation and increase glycolytic energy production during tumorigenesis [1–6]. While this postulate generated a large amount of research over the following decades, technical limitations caused interpretation of the resulting data to be difficult [7]. In spite of decades of research effort, the nature, origin and selective advantage of metabolic alteration in cancer cells remains unclear. In order to take a fresh look at altered cancer metabolism by employing new proteomic technologies, we set out to determine if any differences are observable in the oxidative phosphorylation system between cancer, premalignant and normal cells obtained from the same patient matched tissue specimen.

**Correspondence:** Paul C. Herrmann, FDA-NCI Clinical Proteomics Program, Laboratory of Pathology, National Cancer Institute, 10 Center Drive, Building 10, Room 2N212, Bethesda, MD 20892, USA
**E-mail:** herrmanp@mail.nih.gov
**Fax:** +1-301-480-5005

**Abbreviations: LCM**, laser capture microdissection; **PIN**, prostatic intraepithelial neoplasia

Since the enzyme machinery responsible for oxidative phosphorylation is complicated by being comprised of about 85 individual protein subunits segregated into five main enzyme complexes [8] we chose to focus on only one complex, that of cytochrome *c* oxidase. As the enzyme responsible for the four electron, four proton reduction of oxygen to water, cytochrome *c* oxidase is at the crossroads of oxidative phosphorylation and its kinetic control is essential to oxidative metabolic function [9, 10]. The cytochrome *c* oxidase complex is composed of only thirteen individual protein subunits (see Fig. 1) [11] and is thus amenable to systematic evaluation. Further reducing the complexity is the fact that three subunits (I, II and III) comprise the catalytic core of the enzyme and are all synthesized from mitochondrial DNA. The remaining subunits (IV, Va, Vb, VIa, VIb, VIc, VIIa, VIIb, VIIc and VIII) are synthesized from nuclear DNA found on a variety of chromosomes [12–15] and at least some of these appear to control the kinetic parameters of the core subunits [16–18].

In this study, we evaluate the *in situ* relationship of some nuclear encoded cytochrome *c* oxidase subunit levels to some mitochondrial encoded core subunit levels by immunohistochemistry. We utilize laser capture microdissection (LCM) to procure normal, premalignant and cancerous cells from individual patient matched prostate tissue specimens as well as cells from selected other can-

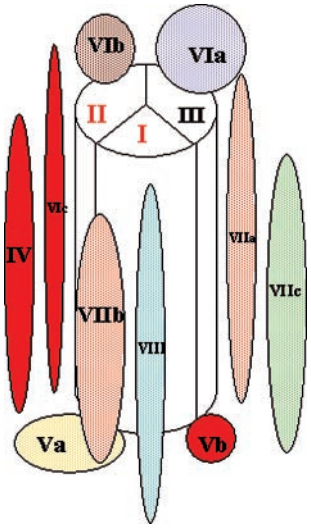


**Figure 1.** Human cytochrome *c* oxidase is composed of 13 individual subunits. The core subunits (I, II, III) represented in white are entirely encoded in the mitochondrial genome and compose the catalytic core of the enzyme. The remaining subunits (IV, Va, Vb, VIa, VIb, VIc, VIIa, VIIb, VIIc, VIII) represented by various colors are encoded in the nuclear genome.

cers [19, 20]. Procuring such cells allows us to evaluate differences in cytochrome *c* oxidase nuclear encoded to mitochondrial encoded subunit level ratios between pure populations of cancer, premalignant and normal cells obtained from the same patient. Moreover, with the use of a new type of protein lysate array [21] we were able to quantify differences in these protein subunit level ratios using the LCM procured cell populations.

## 2 Materials and methods

### 2.1 Specimens

Radical prostatectomy samples ($n$ = 30) were obtained from men that presented with localized prostate cancer. All cases contained carcinoma cells along with various combinations of normal, hypertrophic and premalignant prostatic intraepithelial neoplasia (PIN) tissue on the same microscope slide. Additional data to evaluate the attributability of the findings as a generality of cancer *versus* unique changes associated specifically with prostate tissue were obtained from a variety of nonprostatic human cancer specimens ($n$ = 6). These specimens included three cases of esophageal squamous cell carcinoma, one case of colon adenocarcinoma, one case of breast ductal carcinoma and one case containing ovarian cancer of low metastatic potential as well as carcinoma. All specimens contained normal cells along with cancer cells on the same microscope slide.

### 2.2 Antibodies

Monoclonal mouse antibodies with reactivity to human cytochrome *c* oxidase subunits I, II, IV, Vb and VIc were purchased from Molecular Probes (Eugene, OR, USA) and diluted to form stock solutions as indicated below with a 1% bovine serum albumin (Sigma, St. Louis, MO, USA), 2 mM sodium azide (Sigma) solution made from Dulbecco's PBS (Gibco BRL, Grand Island, NY, USA). Incubation of all the antibodies with the membranes was performed in I-Block (Tropix, Bedford, MA, USA) overnight at 5°C with the stock solutions diluted in I-Block as described below. Cytochrome *c* oxidase subunit I (Molecular probes catalog number A-6403) was diluted with the BSA solution to a concentration of 2 mg/mL for the stock solution that was used at 1:100 dilution in I-Block for membrane incubation. Cytochrome *c* oxidase subunit II (Molecular probes catalog number A-6404) was diluted with BSA solution to a concentration of 2 mg/mL for the stock solution that was used at 1:100 dilution in I-Block for membrane incubation. Cytochrome *c* oxidase subunit IV (Molecular Probes catalog number A-6409) was diluted with BSA solution to a concentration of 5 mg/mL for the stock solution that was used at 1:1000 dilution in I-Block for membrane incubation. Cytochrome *c* oxidase subunit Vb (Molecular Probes catalog number A-6456) was diluted with BSA solution to a concentration of 3 mg/mL for the stock solution that was used at 1:100 dilution in I-Block for membrane incubation. Cytochrome *c* oxidase subunit VIc (Molecular Probes catalog number A-6401) was diluted with BSA solution to a concentration of 2 mg/mL for the stock solution that was used at 1:100 dilution in I-Block for membrane incubation.

Monoclonal mouse antibody to human beta-actin (Alpha Diagnostics cat#ACTB12-M antibody #2; San Antonio, TX, USA) was purchased. This antibody is packaged as ascitic fluid that was used at 1:1000 dilution in the I-Block solution described above for membrane incubation. Goat polyclonal anti-mouse alkaline phosphatase conjugated antibody (Applied Biosystems cat#AC32ML; Bedford, MA, USA) was purchased and used at 1:5000 dilution in the I-Block solution described above for membrane incubation.

### 2.3 Immunohistochemistry

We performed immunohistochemical staining with antibodies to the cytochrome *c* oxidase mitochondrial encoded subunits I and II and the cytochrome *c* oxidase nuclear encoded subunits IV, Vb, and VIc on a series of microscope slide specimens from a single case (PR9827, Fig. 2). The immunohistochemistry was performed with the DAKO envision + system according to

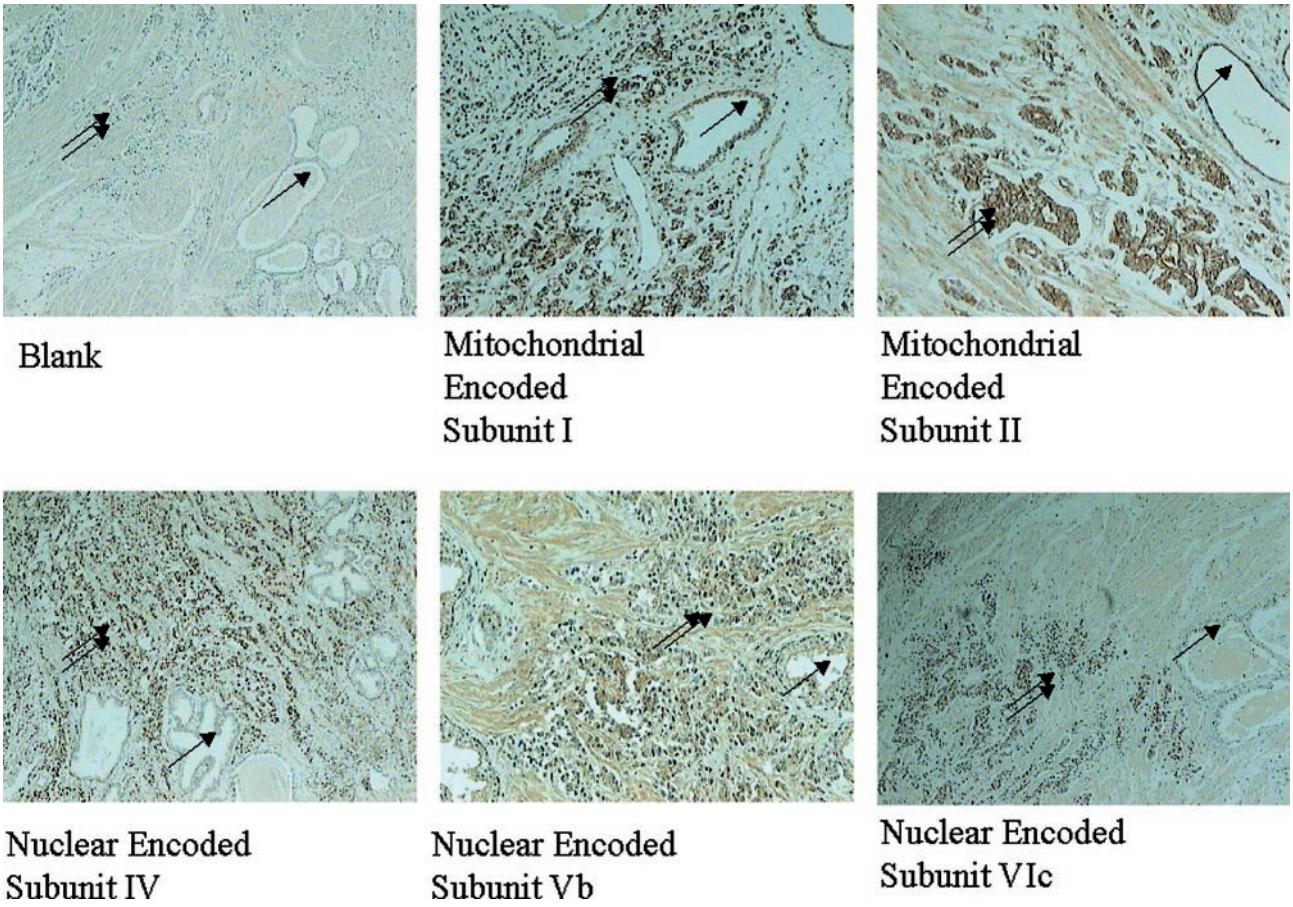


**Figure 2.** Immunohistochemical analysis of subunit intensities of case PR9827. Serial sections of tissue from the same patient have been stained by immunohistochemical methodology with antibodies to the cytochrome *c* oxidase subunits indicated. A single arrow marks a representative area of noncancerous glandular epithelium. A double arrow marks a representative area of cancerous glandular epithelium. Note the intensity of cancer cell staining to noncancerous cell staining in each panel.

the DAKO protocol (DAKO, Carpinteria, CA, USA). The antibody probes were used exactly according to the recommended guidelines supplied by Molecular Probes for immunohistochemical studies. An additional 25 specimens were immunohistochemically stained with antibodies to the mitochondrial encoded subunit II and the nuclear encoded subunit IV of cytochrome *c* oxidase.

### 2.4 Sample selection

Of the 30 cases described in Section 2.1, a selection was made of cases which contained adequate quantities of normal, tumor and in some cases premalignant tissue such as PIN to allow microdissection of the various tissue types from the same microscope slide in sufficient quantities for both Western blot and reverse phase protein microarray analysis. This corresponds to a minimum requirement of approximately 8000 cells of each tissue type for Western blot and 2000 cells of each tissue type for reverse phase protein microarray analysis.

### 2.5 Sample preparation

Tissue specimens were obtained from whole prostate organ mounts that had been fixed with ethanol and embedded in paraffin. Complete prostate cross-sections were obtained by microtome from each specimen and a standard microscope slide was prepared. All nonprostate specimens were paraffin embedded samples that had been fixed in ethanol. Each slide was stained with hematoxylin for cell identification as follows. The slide with mounted paraffin embedded tissue was soaked in xylene for 30 min. The slide was then placed in 70% ethanol for 2 min, rinsed with water, placed in Mayer's 0.1% hema-

toxylin solution (Sigma) for 1.5 min and rinsed with water. The slide was then placed in blueing solution (Fisher Scientific, Pittsburgh, PA, USA) for 30 s followed by desiccation through solutions of 70%, 95% and absolute ethanol. Following desiccation, the slide was immersed in xylene and air-dried. Microdissection of the tissue from the slide was then performed with a Pixcell II LCM system purchased from Arcturus Engineering (Mountain View, CA, USA) according to the published protocol [19]. Samples of normal, prostatic intraepithelial neoplasia (PIN), hypertrophic and tumor tissue were obtained from the same slide and snap-frozen for storage at −80°C. The captured cells were lysed with 1:1 total protein extraction reagent (TPER) (Pierce, Rockford, IL, USA): 2X reducing sample buffer (Novex, San Diego, CA, USA) at 70°C for 2 h and stored at −80°C prior to protein content evaluation.

## 2.6 Western blot analysis

After denaturation at 100°C for 5 min in the same solution the cells were lysed in, the lysates were electrophoresed on polyacrylamide gel electrophoresis (PAGE) 10–20% tris-glycine electrophoresis gels (Novex) at a constant potential of 200 V for 60 min with a Novex E19001-Xcell II mini cell using a standard running buffer (1% SDS, 192 mM glycine, 25 mM Tris). Standard Western blotting onto Immobilon-P (Millipore, Bedford, MA, USA) PVDF membranes was performed at 15 V held constant for 90 min with a Bio-Rad semidry blotter (Hercules, CA, USA) using a standard transfer buffer (20% methanol, 0.037% SDS, 39 mM glycine, 48 mM Tris). The resulting membranes were stained for total protein using Ruby Blot technology (Molecular Probes) according to the vendor-supplied method. The membranes were then blocked with I-Block (Tropix) exactly as directed in the vendor literature. The resulting blots were probed overnight with antibodies for cytochrome *c* oxidase subunits I, II, IV, Vb and VIc (Fig. 3) in antibody containing I-Block solutions as described in Section 2.2. The resulting antibody-bound membranes were then incubated in an I-Block solution of goat anti-mouse alkaline phosphatase conjugated antibodies for 2 h at 5°C as described in Section 2.2. Antibody binding was evaluated by CDP-Star technology (Tropix) exactly as specified in the vendor-supplied instructions. The probed signal was detected by chemiluminescence using Kodak Biomax MR film and the film scanned on a UMAX Powerlook III scanner utilizing Magicscan software.

Since the bands for actin and cytochrome *c* oxidase subunit I are very near each other on Western blots, actin probing was performed after stripping away the other antibodies. The membranes were stripped exactly according to the method described in the Tropix published protocol. The membranes were then reblotted with I-block as described above and probed with the antibody for actin at 5°C for 2 h at the concentration specified in Section 2.2. The remainder of the antibody detection procedure was performed exactly as described above. The scanned images were quantified using ImageQuant software (Amersham Biosciences, Little Chalfont, Bucks, England), signal intensities of the probed proteins were determined, and various subunit ratios were calculated within each single lane. The subunit ratios obtained were analyzed by statistical methods using Microsoft Excel software to yield an average value with a standard deviation. *P*-values between differing ratios were also calculated (see Section 2.8).

## 2.7 Reverse phase protein lysate array analysis

The lysate obtained in the sample preparation section was directly applied to Genetix Fast Slide nitrocellulose membranes (Genetix, Christchurch, Dorset, UK), utilizing a GMS 417 Pin Arrayer (Affymetrix, Redwood, CA, USA) as previously described [21]. Briefly, each LCM-procured lysate was arrayed as a single row of spots (measuring 300 microns *per* spot) for each specimen. Each row consisted of a dilution curve plotted so that each spot in the row had 1/2 the sample quantity of the immediately adjacent spot to its left (the arrayed membranes were then stored at −20°C if not probed immediately). Sequential, identical membranes were blocked with I-block and probed with antibodies to cytochrome *c* oxidase subunits II, IV and Vb (Fig. 3) by immersing each membrane in a bath of the appropriate antibody and buffer solution under conditions identical to those used for Western blot probing described in Section 2.6. Only these three cytochrome *c* oxidase subunit antibodies were probed since they were the only three with absolute specificity for a single band as determined by Western blot analysis. The probed signal was detected by the catalyzed signal amplification (CSA) system from DAKO. After staining, the slides were scanned on a UMAX Powerlook III Scanner utilizing Magicscan software and the spot intensities quantified. The signal intensities were used to obtain intensity values for each of the dilution curves in a region of linear dynamic range by linear regression analysis. Intensity ratios were then determined for each antibody pair as performed for the Western blot analysis. Statistical analysis yielded the average value and standard deviation for each ratio along with *P*-values for differing ratios (see Section 2.8). A direct comparison of the background staining intensity for each experiment was performed by analysis of duplicate experimental slides incubated with the biotinylated secondary antibody alone.

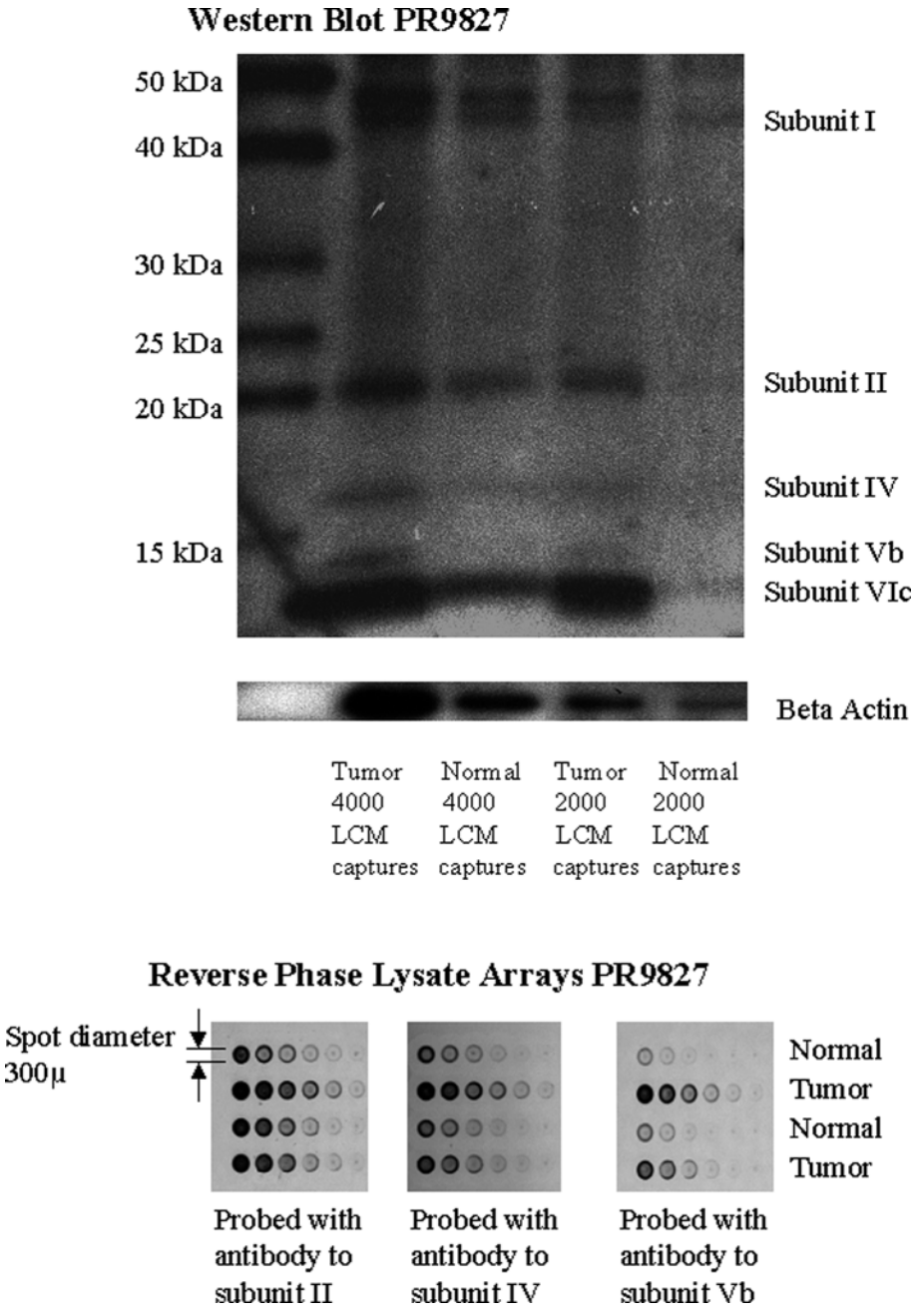


**Figure 3.** Western blot and reverse phase protein lysate array of prostate protein of case PR9827. The upper panel is a picture of a Western blot obtained by serial blotting of antibodies to each cytochrome *c* oxidase subunit indicated. The left most column is a standard molecular weight ladder highlighted by nonspecific protein binding by multiple antibodies. The other four columns are composed of protein from normal and cancerous cells obtained from the same histology section. The number of LCM captures is indicated under each lane (one capture corresponds to approximately four cells). Underneath the cytochrome *c* oxidase subunit probed membrane is the actin pattern obtained from the same membrane after membrane stripping. The bottom three panels are identical reverse phase lysate arrays made from protein removed from a single histological section. Each row is composed of a dilution titration curve in which each spot contains 1/2 the protein content of the spot immediately to its left. The rows are marked to the right, indicating the tumor or normal cell protein origin in each row. The array in each panel was probed with antibody to the cytochrome *c* oxidase subunit indicated underneath. Each lysate array spot is 300 µ in diameter.

### 2.8 Calculations/quantitation

#### 2.8.1 Western data

The data image from each Western blot analysis was opened using ImageQuant software (Amersham Biosciences). The appropriate bands were identified and the integrated pixel intensity of each band was recorded as the raw intensity value for the band. A region of the same dimensions as the quantified band was identified and the integrated pixel intensity of this region was recorded as background intensity. Final band intensity values were obtained by subtracting the background intensity from the raw intensity value of each band.

#### 2.8.2 Reverse phase protein lysate array data

The data image from each reverse phase protein lysate array membrane was scanned into a computer and opened with ImageQuant software as described in Section 2.8.1. The spots were identified and the integrated

pixel intensity of each spot determined. For each series of spots constituting a dilution curve, a plot was made of spot intensity *versus* relative protein concentration. The linear dynamic range portion of the curve was fit to the equation y = mx + b. The intensity of each spot is composed of a component that varies with protein concentration (m in equation y = mx + b) and a component that is fixed irrespective of protein concentration (b in equation y = mx + b). The unchanging component (b in equation y = mx + b) was assumed to be background and the changing quantity (m in equation y = mx + b) was treated as the final intensity value for each dilution curve. In the absence of a dilution curve, it is impossible to determine how much of the given intensity is independent of the protein content and hence background or artifact secondary to nondynamic effects. Consequently, we consider the Western blot data to be less precise and less accurate than that obtained by reverse phase protein lysate array analysis.

### 2.9 Mitochondrial staining

LCM captured cells were stained for mitochondria with Mitotracker Green FM fluorescent mitochondrial stain (Molecular Probes cat#M-7514). The adherent dissected cells were exposed for 15 min to a 1.0 μM Mitotracker Green FM solution. (The Mitotracker solution was prepared by dissolving 50 μg Mitotracker Green FM in 74 mL DMSO to make a stock solution. The stock solution was then diluted 1000-fold with Dulbecco's PBS (GIBCO BRL) to yield the final Mitotracker concentration). The resulting fluorescent signal was scanned with a Vistra Fluorescence Fluorimeter SI using ImageQuant software and the signal quantitated yielding relative mitochondrial concentrations. The stained cells were then lysed as described in Section 2.8.2 and the methods of Western blot analysis and reverse phase protein lysate array continued. The specificity of Mitotracker green FM was determined by staining a blood smear. Only the nonerythrocyte cell populations containing mitochondria fluoresced.

## 3 Results

### 3.1 Immunohistochemistry

Immunohistochemical staining was performed on a total of 26 individual cases of prostate cancer. Photomicrographs of a single immunohistochemically stained case (PR9827) along with the negative control are shown in Fig. 2. These images show very slightly decreased intensity of cytochrome *c* oxidase mitochondrial encoded subunit (subunits I and II) staining and significantly increased intensity of cytochrome *c* oxidase nuclear encoded subunit (subunits IV, Vb and VIc) staining of cancerous cells compared with normal glandular cells on the same microscope slide. The additional 25 cases all yielded identical results (data not shown for 25 cases).

### 3.2 Western blot analysis

Western blot analysis was performed on a total of four cases of prostate cancer. Each case was selected to contain at least 8000 tumor and 8000 nontumor cells on a single microscope slide. Two cases (PR9827, PR001) contained ample tissue, well in excess of this requirement. The other two cases (PR9875, 317) contained barely enough tissue of the two types to meet the above requirement. Hence, not all the probed bands of cases PR9875 and 317 yielded intensities adequate to distinguish subunit intensities from background staining for these two cases.

The proteins applied to the Western blot were microdissected and solubilized from the above described sections. Antibodies to subunits II, IV and Vb showed specificity to single bands. Antibodies to subunits I and VIc showed moderate nonspecific binding and consequently these bands were assigned based on staining as well as molecular weight location on the membranes. The antibody probed intensities of the mitochondrial encoded cytochrome *c* oxidase subunits I and II, and the probed intensities of the nuclear encoded cytochrome *c* oxidase subunits IV, Vb and VIc normalized to actin and total protein are shown in Table 1 and a representative graph for one case (PR001) is shown in Fig. 4 (see Section 2.8 for description of quantitation methods). A representative Western blot of one case (PR9827) is shown in Fig. 3. These results demonstrate increased nuclear encoded cytochrome *c* oxidase subunit intensity and decreased or unchanged mitochondrially encoded cytochrome *c* oxidase subunit intensity in cancer compared with normal tissue. These intensity changes result in an increase in the ratio of nuclear encoded cytochrome *c* oxidase subunits to mitochondrial encoded cytochrome *c* oxidase subunits commensurate with cancer. The ratios of cytochrome *c* oxidase subunits I to II are not statistically different ($P > 0.9$) on comparison of normal and tumor tissue, providing an internal control. Since both subunits are transcribed together from the circular monocistronic mitochondrial DNA molecule, their production ratio should always be fixed [22, 23].

### 3.3 Reverse phase protein lysate array analysis

Reverse phase protein lysate array analysis was performed on a total of four prostate cases and six nonprostatic cancer cases. Cases were selected which con-

**Table 1.** Prostate protein intensity data obtaind by Western analysis

| Case | Ratios | | | | Normalized to actin and total protein | | | | |
|---|---|---|---|---|---|---|---|---|---|
| | IV/II | Vb/II | VIc/II | II/I | I | II | IV | Vb | VIc |
| PR9827 | | | | | | | | | |
| normal | **0.41** | **0.19** | **1.31** | **1.34** | **0.39** | **0.55** | **0.22** | **0.10** | **0.76** |
| std | 0.14 | 0.04 | 0.39 | 0.32 | 0.17 | 0.33 | 0.12 | 0.04 | 0.51 |
| tumor | **0.85** | **0.66** | **2.93** | **1.39** | **0.38** | **0.49** | **0.41** | **0.31** | **1.43** |
| std | 0.27 | 0.21 | 0.58 | 0.34 | 0.13 | 0.08 | 0.12 | 0.05 | 0.28 |
| PR001 | | | | | | | | | |
| normal | **0.12** | **0.18** | **0.16** | **0.94** | **0.31** | **0.29** | **0.036** | **0.052** | **0.046** |
| std | 0.01 | 0.01 | 0.01 | 0.05 | 0.02 | 0.01 | 0.002 | 0.003 | 0.002 |
| tumor | **0.22** | **0.42** | **0.38** | **0.93** | **0.32** | **0.30** | **0.065** | **0.126** | **0.113** |
| std | 0.01 | 0.02 | 0.02 | 0.05 | 0.02 | 0.02 | 0.003 | 0.006 | 0.006 |
| PR9875 | | | | | | | | | |
| hypertrophy | **0.15** | **0.043** | N/A | N/A | N/A | **1.54** | **0.23** | **0.066** | N/A |
| std | 0.01 | 0.004 | | | | 0.15 | 0.02 | 0.007 | |
| tumor | **0.71** | **0.31** | N/A | N/A | N/A | **0.86** | **0.62** | **0.27** | N/A |
| std | 0.07 | 0.03 | | | | 0.09 | 0.06 | 0.03 | |

| 317 | IV/I | VIc/I | I | IV | VIc |
|---|---|---|---|---|---|
| normal | **0.328** | **0.32** | **1.23** | **0.41** | **0.36** |
| std | 0.007 | 0.10 | 0.47 | 0.16 | 0.04 |
| tumor | **1.35** | **0.96** | **0.50** | **0.66** | **0.48** |
| std | 0.24 | 0.23 | 0.18 | 0.12 | 0.07 |

The table shows actin and total protein normalized intensity values of cytochrome *c* oxidase subunits obtained by Western blot analysis and corresponding calculated ratios. Numbers shown in **bold** are an average of at least three independent measurements. The SD's are shown in light type. The differences for a given ratio within each case all yield *P*-values $< 0.02$. Data unobtainable due to insufficient protein content are indicated with N/A.

tained at least 2000 cells of each tissue type to be evaluated on a single microscope slide. Two thousand or more cells of each tissue type were then dissected from each microscope slide, lysed and applied in a separate dilution curve to reverse phase protein lysate array membranes as previously described. The relative cytochrome *c* oxidase subunit concentrations were determined as described in Section 2.8.2. The utilization of a dilution curve allows much more accurate and precise quantitative analysis then does the Western blot, but maintains the advantage of patient matched analysis with decreased inter-sample variability obtained by dissecting all tissue types from a single microscope slide. Tissue types evaluated included normal and tumor prostate, PIN, prostatic hypertrophic tissue, ovarian tissue of low malignant potential as well as carcinomas of the ovary, esophagus, colon and breast.

Cytochrome *c* oxidase subunits II, IV and Vb were probed under identical conditions described for Western blotting. Of the antibodies to cytochrome *c* oxidase subunits available, only these three showed single protein band specificity by Western blotting and consequently were the only ones appropriate for reverse phase protein lysate array analysis. Antibodies with high specificity are required for reverse phase protein lysate array analysis, since this technique does not separate proteins prior to antibody probing.

The intensity ratios of the nuclear encoded cytochrome *c* oxidase subunits IV and Vb to the mitochondrially encoded cytochrome *c* oxidase subunit II for the prostate cases are shown in Table 2 and a representative graph for one case (PR0011) is shown in Fig. 4. The probed membranes for a single case (PR9827) are shown in Fig. 3. The data from the nonprostatic cases are tabulated in Table 3. A progressive increase in the ratio beginning very early in cancer progression is clearly demonstrated as the normalized intensity values are elevated in the patient-matched PIN lysates. Plotting a dilution curve of the lysate demonstrates that the observed ratio effects are present in regions of linear dynamic range and not an artifact of probing nonlinear dynamic ranges.

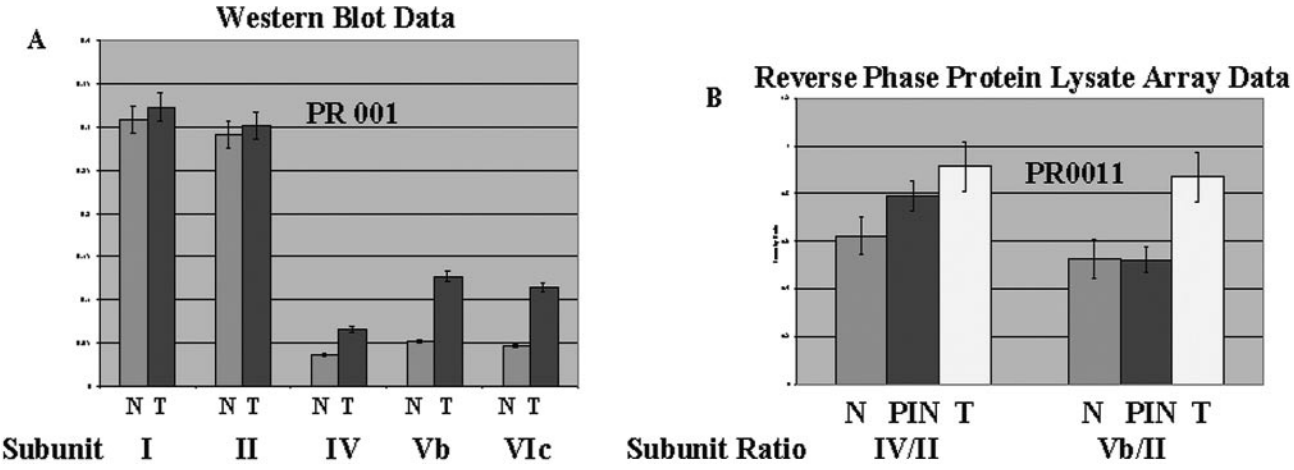


**Figure 4.** A shows a graph of representative data obtained by Western blot analysis. The intensities of the Western blot data are shown as the intensities normalized to actin and total protein. B shows a graph of representative data obtained by the reverse phase protein microarray technique. The intensity data are shown as a ratio of the cytochrome *c* oxidase nuclear encoded subunit intensity indicated relative to the mitochondrial cytochrome *c* oxidase subunit II intensity. The case numbers are indicated on the individual graphs and correspond to the data listed in Tables 1 and 2 for each case. N = normal tissue, T = tumor tissue, PIN = prostatic intraepithelial neoplasia tissue.

In the absence of a dilution curve it is impossible to determine how much of the given intensity is independent of the protein content and hence background or artifact secondary to nondynamic effects. Consequently, we consider the Western blot data to be less precise and accurate than that obtained by reverse phase protein lysate array analysis. The methods of evaluation utilized in evaluating the data make comparison of absolute values obtained by Western blot with those obtained by reverse phase protein lysate array impossible (see Section 2.8). Both methods do demonstrate identical trends, however. The independence of these observable trends from the methods of evaluation yields credence to the trend's existence while the data obtained by reverse phase protein lysate array yield more precise and accurate assessment of the trend.

### 3.4 Mitochondrial staining

Staining intensity values were obtained with Mitotracker Green FM mitochondrial stain (Molecular Probes) along with Western blot analysis of total protein and actin for a single case (PR9827). The intensity ratios of tumor cell to normal cell mitochondrial mass, total protein and actin were determined for this case. The results were obtained by three independent evaluations of the same case and the averages calculated along with SD's for each probe. The ratios of tumor : normal mitochondrial mass, tumor : normal protein content and tumor : normal actin content are all between 3.4 and 4.2 with no statistically significant differences between them. These results indicate that mitochondrial mass, total protein and actin content of the cells evaluated are all covariate and imply that the observed changes in subunit intensities we observe are not simply a consequence of altered cellular mitochondrial mass between tumorous and normal cells.

## 4 Discussion

We have employed LCM technology coupled with downstream proteomic platforms *via* a new type of protein array to identify a previously unknown cancer-associated shift in the ratio of nuclear encoded cytochrome *c* oxidase subunits IV, Vb and VIc relative to mitochondrial encoded cytochrome *c* oxidase subunits I and II directly from human cancer tissue specimens. The association with cancer was confirmed in 36/36 specimens ($P < 0.001$) we examined, indicating a ubiquitous change.

We utilized LCM to microdissect tissue for comparison from a single microscope slide, yielding the lowest possible variability between tissue types compared. The cancer associated subunit shift was observed with immunohistochemistry, crudely quantified by Western blot and quantitatively refined by reverse phase protein lysate array. While the methods presented demonstrate the presence of the cancer associated trend by tissue section immunohistochemistry, Western blot and reverse phase protein lysate array, it is our contention that data analysis precise and accurate enough to distinguish differences between premalignant conditions such as PIN and invasive carcinoma requires dilution curve analysis and low

**Table 2.** Prostate protein intensity data obtained by reverse phase protein lysate array methodology

| Case | Ratios | |
|---|---|---|
| | IV/II | Vb/II |
| PR9827 | | |
| normal | **0.178** | **0.16** |
| std | 0.009 | 0.02 |
| carcinoma | **0.59** | **0.30** |
| std | 0.10 | 0.08 |
| PR0011 | | |
| normal | **0.62** | **0.53** |
| std | 0.08 | 0.08 |
| PIN | **0.79** | **0.52** |
| std | 0.06 | 0.05 |
| carcinoma | **0.91** | **0.87** |
| std | 0.10 | 0.10 |
| PR001 | | |
| normal | **0.17** | **0.44** |
| std | 0.05 | 0.09 |
| hypertrophy | **0.44** | **0.44** |
| std | 0.04 | 0.05 |
| PIN | **0.66** | **0.40** |
| std | 0.12 | 0.08 |
| carcinoma | **1.11** | **0.55** |
| std | 0.10 | 0.06 |
| PR9875 | | |
| normal | **4.14** | **5.84** |
| std | 0.24 | 0.36 |
| PIN | **13.4** | **10.5** |
| std | 0.8 | 0.9 |
| carcinoma | **12.9** | **8.4** |
| std | 2.3 | 1.5 |

The table shows intensity ratios of nuclear encoded to mitochondrial encoded cytochrome *c* oxidase subunits obtained by reverse phase protein lysate array analysis. The numbers shown in **bold** are averages obtained from a minimum of five measurements for each cytochrome *c* oxidase subunit. The SD's are shown below each value. The differences for a given ratio within a single case all yield *P*-values $< 0.02$.

cellular mass requirements untenable by standard Western blot analysis alone. We consequently employed the reverse phase protein lysate array analysis to observe these differences after determining which anti-cytochrome *c* oxidase subunit antibodies are specific for a single protein band by Western blot analysis.

Of particular importance is the observation that these subunit differences begin to appear very early in prostatic premalignant conditions such as PIN and increase in magnitude as the carcinoma cells become invasive. These changes are independent of mitochondrial mass, total protein and cellular actin content. This is significant since evidence implicates the nuclear encoded subunits IV, Vb and VIc in the kinetic control of cytochrome *c* oxidase [17]. Of particular relevance are the findings that some of this control is exerted through relative concentrations of subunits IV and VIc [16].

If the concentrations of the nuclear subunits relative to mitochondrial encoded subunits do control the Km, then the changes in the ratios that we observe must alter the rate of oxidative metabolism in prostate cells during tumorigenesis. Such an alteration may not be a direct consequence of cancer, however. Prostate metabolism is unique. In normal prostate tissue, the Krebs cycle enzyme aconitase is inhibited by high zinc concentrations. This diverts metabolic intermediates such as citrate away from the Krebs cycle, decreasing the yield of metabolism to about 14 ATP *per* glucose [24] instead of the usual quantity of about 36 [25]. Once the prostate tissue becomes cancerous, the inhibition of aconitase ceases, increasing the amount of ATP produced *per* single glucose molecule [26].

The increased ratios of nuclear to mitochondrial cytochrome *c* oxidase subunits we observe upon tumorigenesis could be a response by the prostate cancer cells to the increase in reducing-equivalents feeding into the electron transport system from the altered Krebs cycle rather then from cancer. To determine if the observed effects were actually due to cancer, we evaluated a small number of nonprostatic cancer cases by protein reverse phase lysate array analysis to determine whether or not the observed results were unique to prostate cancer. The results are shown in Table 3 for a variety of cancers and demonstrate the same trends, implying that the changes are associated with carcinoma in general and are not unique to the prostate. Thus, these data may imply a generalized cancer mechanism, which causes an increased rate of neoplastic oxidative phosphorylation relative to normal tissue. Such a change might give cells early in their conversion to cancer, a selective advantage over normal cells. The results we obtained by measuring protein subunit levels viewed in conjunction with reports of increased mRNA levels of some of the same subunits in a variety of cancerous tissues [27–32] suggests that the effect results from increased production rates of the nuclear encoded cytochrome *c* oxidase subunits rather than decreased subunit breakdown rates.

Such derangements in mitochondrial metabolism may constitute new targets for treatment, based upon a metabolic paradigm. Since the effects are seen in the earliest premalignant lesions associated with prostate cancer such an approach would permit therapy effective very early in disease progression. Such early observable effects also suggest that cytochrome *c* oxidase subunit

**Table 3.** Protein intensity data for a variety of cancer types

| | IV/II | std | Vb/II | std |
|---|---|---|---|---|
| Ovarian tissue | | | | |
| LMP | **0.18** | 0.06 | **0.29** | 0.04 |
| carcinoma | **0.58** | 0.18 | **0.76** | 0.12 |
| Colon tissue | | | | |
| normal | **0.22** | 0.02 | **1.07** | 0.08 |
| adenocarcinoma | **0.43** | 0.01 | **1.22** | 0.04 |
| Esophageal case 1 | | | | |
| normal | **0.124** | 0.007 | **0.41** | 0.03 |
| carcinoma | **0.16** | 0.02 | **0.65** | 0.12 |
| Esophageal case 2 | | | | |
| normal | **0.10** | 0.02 | **0.49** | 0.07 |
| carcinoma | **0.39** | 0.04 | **0.70** | 0.05 |
| Esophageal case 3 | | | | |
| normal | **0.05** | 0.02 | **0.61** | 0.10 |
| carcinoma | **0.13** | 0.03 | **0.75** | 0.06 |
| Breast tissue | | | | |
| normal | N/A | | **0.22** | 0.03 |
| carcinoma | N/A | | **0.40** | 0.03 |

Intensity ratios of nuclear encoded to mitochondrial encoded subunits obtained by reverse phase protein lysate array analysis. The numbers shown in **bold** are averages obtained from a minimum of five measurements for each subunit. The SD's are shown adjacent to each value. The differences for a given ratio within a single case all yield $P$-values $< 0.0375$. The breast cancer case did not yield interpretable results for cytochrome *c* oxidase subunit IV and hence the ratios for subunit IV are not calculable and are indicated as N/A.

ratios may prove valuable as markers of tumor progression, even before histologically observable changes are present.

## 5 Concluding remarks

The use of LCM and reverse phase protein lysate array technology was critical to this analysis. Only through the microdissection and dilution curve analysis of patient matched longitudinal study sets was it possible to demonstrate quantitatively the small alterations in protein levels present in the earliest premalignant lesions. This analysis points to a possible role for nuclear DNA encoded mitochondrial proteins in carcinogenesis, and supports the need for full characterization of the mitochondrial proteome.

Received January 14, 2003
Revised April 7, 2003
Accepted April 7, 2003



## 6 References

[1] Warburg, O., Posenor, K., Negelein, E., *Biochem. Z.* 1924, *152*, 309–345.

[2] Warburg, O., *Science* 1956, *123*, 309–314.

[3] Warburg, O., Kubowitz, F., *Biochem. Z.* 1927, *189*, 242–249.

[4] Warburg, O., Negelein, E., *Biochem. Z.* 1928, *193*, 334–339.

[5] Warburg, O., *Biochem. Z.* 1929, *204*, 482–494.

[6] Warburg, O., *Metabolism of Tumors*, Arnold Constable, London 1930.

[7] Pedersen, P. L., *Prog. Exp. Tumor Res.* 1978, *22*, 190–274.

[8] Scheffler, I. E., *Mitochondria*, Wiley-Liss, New York 1999.

[9] Groen, A. K., Wanders, R. J., Westerhoff, H. V., van der Meer, R., Tager, J. M., *J. Biol. Chem.* 1982, *257*, 2754–2757.

[10] Villani, G., Attardi, G., *Free Radic. Biol. Med.* 2000, *29*, 202–210.

[11] Tsukihara, T., Aoyama, H., Yamashita, E., Tomizaki, T. *et al*., *Science* 1996, *272*, 1136–1144.

[12] Hofmann, S., Lichtner, P., Schuffenhauer, S., Gerbitz, K. D., Meitinger, T., *Cytogenet. Cell Genet.* 1998, *83*, 226–227.

[13] Lee, N., Morin, C., Mitchell, G., Robinson, B. H., *Biochim. Biophys. Acta* 1998, *1406*, 1–4.

[14] Arnaudo, E., Hirano, M., Seelan, R. S., Milatovich, A. *et al*., *Gene* 1992, *119*, 299–305.

[15] Hey, Y., Hoggard, N., Burt, E., James, L. A., Varley, J. M., *Cytogenet. Cell Genet.* 1997, *77*, 167–168.

[16] Vijayasarathy, C., Biunno, I., Lenka, N., Yang, M. *et al*., *Biochim. Biophys. Acta* 1998, *1371*, 71–82.

[17] Kadenbach, B., Huttemann, M., Arnold, S., Lee, I., Bender, E., *Free Radic. Biol. Med.* 2000, *29*, 211–221.

[18] Yanamara, W., Zhang, Y. Z., Takamiya, S., Capaldi, R. A., *Biochemistry* 1988, *27*, 4909–4914.

[19] Emmert-Buck, M. R., Bonner, R. F., Smith, P. D., Chuaqui, R. F. *et al*., *Science* 1996, *274*, 998–1001.

[20] Liotta, L., Petricoin III, E., *Nat. Rev. Genet.* 2000, *1*, 48–56.

[21] Paweletz, C. P., Charboneau, L., Bichsel, V. E., Simone, N. L. *et al*., *Oncogene* 2001, *20*, 1981–1989.

[22] Anderson, S., Bankier, A. T., Barrell, B. G., de Bruijn, M. H. *et al*., *Nature* 1981, *290*, 457–465.

[23] Andrews, R. M., Kubacka, I., Chinnery, P. F., Lightowlers, R. N. *et al*., *Nat. Genet.* 1999, *23*, 147–147.

[24] Costello, L. C., Franklin, R. B., *Oncology* 2000, *59*, 269–282.

[25] Stryer, L., *Biochemistry 4th Ed*, W. H. Freeman, New York 1995.

[26] Costello, L. C., Franklin, R. B., Liu, Y., Kennedy, M. C., *J. Inorganic Biochem.* 2000, *78*, 161–165.

[27] Yanamoto, A., Horai, S., Yuasa, Y., *Biochem. Biophys. Res. Commun.* 1989, *159*, 1100–1106.

[28] Gromova, I., Gromov, P., Celis, J. E., *Electrophoresis* 1999, *20*, 241–248.

[29] Glaichenhaus, N., Leopold, P., Cuzin, F., *EMBO J.* 1986, *5*, 1261–1265.

[30] Corral, M., Paris, B., Baffet, G., Tichonicky, L. *et al*., *Exp. Cell. Res*. 1989, *184*, 158–166.

[31] Luciakova, K., Kuzela, S., *Eur. J. Biochem.* 1992, *205*, 1187–1193.

[32] Wang, F. L., Wang, Y., Wong, W. K., Liu, Y. *et al*., *Cancer Res.* 1996, *56*, 3634–3637.